BUTTERWORTH
HEINEMANN

Polymer Vol. 36 No. 26, pp. 4919–4925, 1995

0032-3861/95/$10.00+0.00

The effect of high-intensity ultrasound on solid polymers

Gareth J. Price*, Amanda J. White and Andrew A. Clifton
School of Chemistry, University of Bath, Claverton Down, Bath BA2 7AY, UK
(Received 25 November 1994; revised 27 April 1995)

Powders of polyethylene, polypropylene, poly(vinyl chloride) and poly(methyl methacrylate) have been subjected to irradiation with high-intensity ultrasound while suspended in water. Changes in the particle sizes and the surface morphology were noted and the pattern of the results was correlated with the physical properties of the materials. In anticipation of sonochemically enhanced reactions at polymer surfaces, the effect on a polyethylene sheet was also examined. The implications of the results for preparative methods as well as surface reactions are discussed.

(Keywords: polymer particles; ultrasonic irradiation; physical properties)

INTRODUCTION

The past decade has seen a dramatic rise in the applications of high-intensity, or power, ultrasound in chemistry, with a range of synthetic procedures and process methods having been found to benefit from sonication[1–3]. While some of these have been homogeneous systems, study of heterogeneous systems has been more common, and this led to investigation of the effect of ultrasound on particles of inorganic materials such as metals and metal oxides as well as on extended surfaces suspended in liquid[4–6].

The major chemical effects of ultrasound are due to cavitation[7], the rapid growth and explosive collapse of microscopic bubbles as the alternate compression and rarefaction phases of the sound wave pass through the liquid. Depending on the liquid and the precise conditions used, these bubbles will be in the range 100–200 μm in diameter[8] and the collapse can generate enormously high temperatures, pressures and electric fields on a microsecond timescale, as well as generating high shear gradients and shock waves. When a bubble collapses close to a surface, microjets of liquid are produced that impinge on the surface[9] at high velocity and can also set suspended solid particles into motion. Suslick *et al.* showed that small (~5–10 μm) particles of metals collided at speeds approaching 500 m s^{-1} and the collisions generated sufficient energy to melt and fuse the particles at the site of contact[4]. By using metals with a range of melting points, they were able to postulate that local temperatures of the order of 2600–3200 °C resulted at the collision sites. In contrast, sonication of larger particles of inorganic solids such as TaS_2 and MoO_3 resulted[6] in a rapid lowering of the average particle size down to a lower limit of 5–10 μm. Lindley *et al.*[10] reported similar effects for copper powder, with the average particle size being reduced from 87 μm to 23 μm after 1 h sonication, giving a more active catalyst for Ullmann-type reactions.

The best-known effect of power ultrasound in polymer chemistry is the non-random depolymerization of chains in solution[11,12]. More recently[13], sonochemically enhanced methods of polymer synthesis have been described, including radical initiation, emulsion, suspension, ring opening and electrochemical processes. As far as the authors are aware, there has been only one report of the effect of sonicating polymer particles or surfaces, in which Urban and Salazar-Rojas showed[14] that the dehydrofluorination of poly(vinylidene difluoride) to give conjugated surfaces was enhanced by the phase transfer catalyst properties of ultrasound. Given the recent enhanced interest in these synthetic methods, the use of ultrasound for processes such as emulsification and dispersion as well as other potential sonochemical applications such as the production of latexes, chemical functionalization of surfaces and the acceleration of reactions using polymer-supported reagents, it is timely to examine the effect on a range of polymers. We have done this by measuring the effect of sonication on the

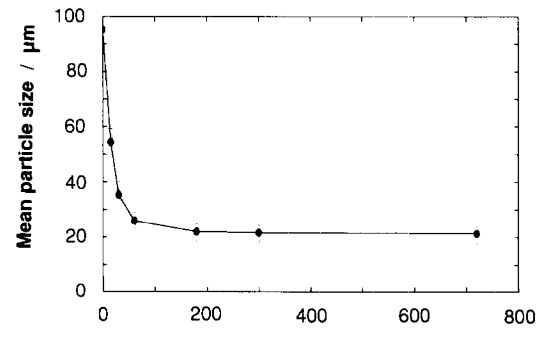

Figure 1 Change in average size for polyethylene particles sonicated at 26.2 W cm^{-2} for 5 h in water at a loading of 3 g/100 cm^3

---

* To whom correspondence should be addressed

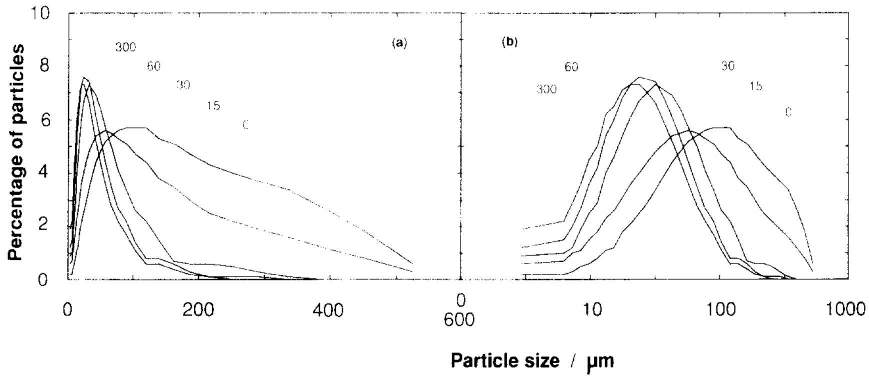

Figure 2 Distribution of particle sizes for sonicated polyethylene powder (conditions as in *Figure 1*): (a) linear plot, (b) logarithmic plot. Sonication times from 0 to 300 min are indicated on the curves

particle size and morphology of particles of several polymers with a range of physical properties as well as on the surface of a polyethylene sheet.

EXPERIMENTAL

Materials

The polymers used in this study were as follows: polyethylene (PE) powder with molecular weight 145 000 supplied by BP Ltd; polypropylene (PP) powder with melt flow index 1.6 supplied by Amoco Ltd; poly(vinyl chloride) (PVC) from Aldrich with inherent viscosity 0.92 and $M_n \sim 177000$; and poly(methyl methacrylate (PMMA) beads with molecular weight 500 000 supplied by BDH Ltd. Polyethylene films with a thickness of 0.2–0.3 mm were prepared by melt pressing the above powder.

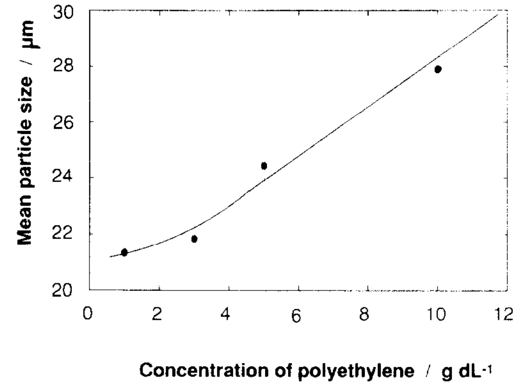

Figure 3 Variation in limiting mean particle size with the mass of polyethylene powder sonicated in 100 cm^3 water (other conditions as in *Figure 1*)

Sonication procedure

Ultrasonic irradiation was carried out using a 'Sonics and Materials' VC600 ultrasound horn system[15]. The intensity used was measured calorimetrically in the usual manner[16] and found to be 26.2 ± 1.3 W cm^{-2}. Distilled water (100 cm^3) was used as the supporting liquid in each case and was contained in a jacketed vessel through which cooling water was circulated to maintain the temperature at 25.0 ± 0.5°C. A weighed amount of the polymer powder was added to the vessel and it was found that sonication provided sufficient agitation to maintain dispersion throughout the liquid. Irradiations on the polyethylene films were carried out by clamping a 2 cm × 2 cm square of the film in a steel holder placed in the water at a fixed distance from the tip of the horn.

Analytical techniques

Particle sizes were determined with a Malvern Instruments 2600c Autosizer operated in 'easy' mode. Measurements were made using lenses with focal lengths of 100 mm or 300 mm, giving particle-size results in the ranges 1.9–188 µm and 5.8–564 µm respectively. A 2 mm path length cell was used with a supporting liquid of 95/5 ethanol/water to obtain wetting of the particles. The results were calculated according to the 'log-normal' distribution method and are shown below as the number percentage

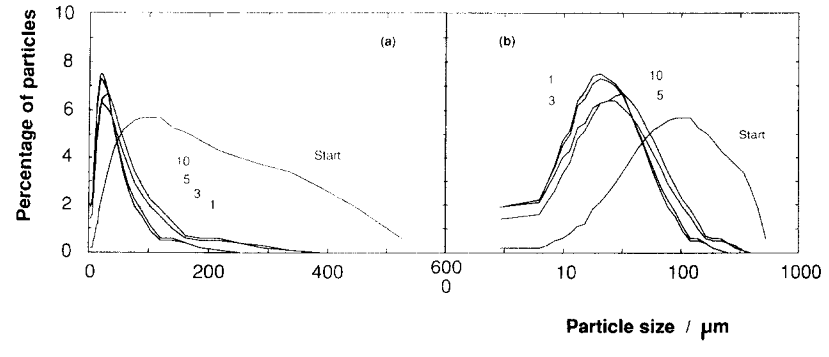

Figure 4 Distribution of particle sizes for sonicated polyethylenes at various loadings, as in *Figure 3*: (a) linear plot, (b) logarithmic plot. Polyethylene loadings from the starting distribution to 10 g/100 cm^3 are indicated on the curves

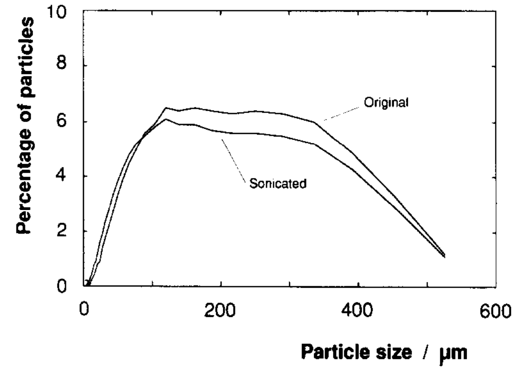

Figure 5 Change of particle size distribution by 5 h sonication of the first sample of polypropylene powder (conditions as in *Figure 1*)

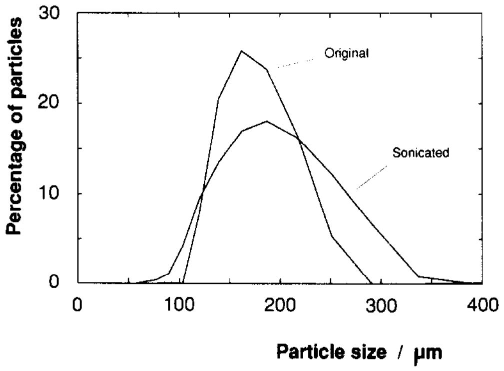

Figure 8 Change in the distribution of particle sizes for sonicated poly(vinyl chloride) (conditions as in *Figure 1*)

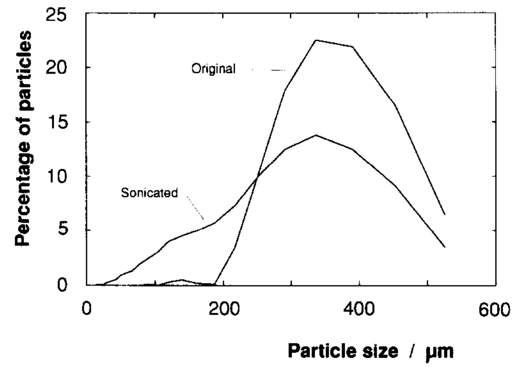

Figure 6 Change of particle size distribution by 5 h sonication of the second sample of polypropylene powder (conditions as in *Figure 1*)

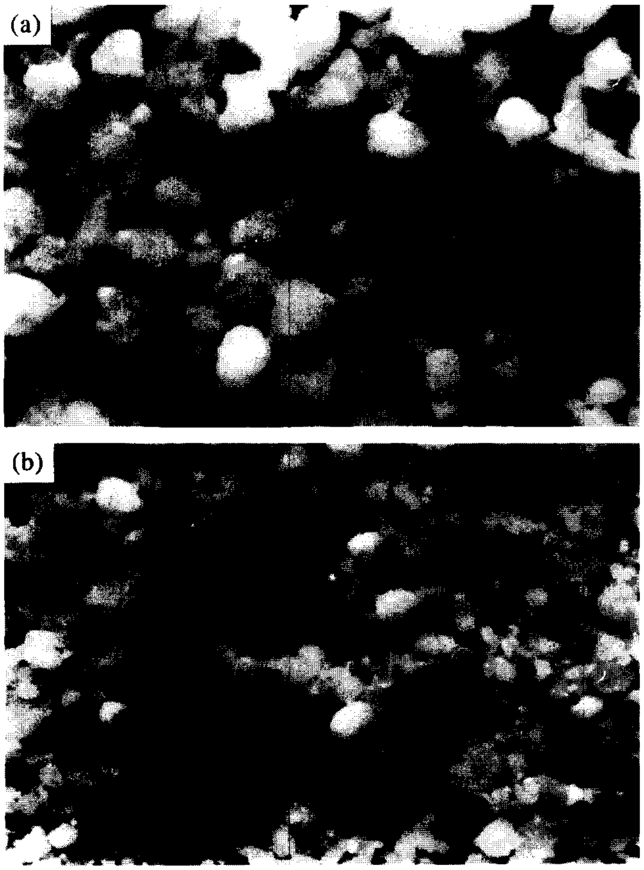

Figure 7 Optical micrographs (magnification ×25) of polypropylene samples from *Figure 6*: (a) before sonication, (b) after sonication

of the total sample falling into particular size ranges. Optical microscopy was carried out with a Zeiss Stemi SVII microscope allowing a magnification typically up to 70 ×. Electron micrographs were recorded with a JEOL T330 scanning electron microscope on samples coated with gold using an Edwards S150B sputter coater.

RESULTS AND DISCUSSION

The first polymer studied was a commercial, low-density polyethylene sample supplied with an average particle size of 94 μm. *Figure 1* shows the change of particle size with sonication time and demonstrates the initially rapid lowering that levelled to a limiting value of 21 μm below which no further change was apparent. It thus has features similar to the degradation process of individual chains in solution[11,12], although the mechanism giving rise to the effect is different. Further information can be gained from considering the changes in the distribution of particle sizes shown in *Figure 2*. Particles larger than ~ 100 μm were broken up very quickly and virtually disappeared from the plot after 30 min. The behaviour at small sizes is more clearly seen when the logarithm of the size is plotted as in *Figure 2b*. Particles smaller than ~ 5 μm were unaffected.

Two effects could be responsible for the particle rupture. First, the microstreaming of liquid jets and shock waves impinging on the particle could set up stresses within the solid and lead to fragmentation. Alternatively, rupture could arise as a result of interparticle collisions. In this case, microjets arising from cavitation bubbles of diameter 150–200 μm would be significantly larger than the particles so that it is more likely that the powder would be set into motion rather than absorbing the shock and fragmenting directly. To assist in interpreting the results, sonications were carried out with a range of polymer loadings, and the results after 5 h sonication are shown in *Figures 3* and *4*.

Figure 3 shows that there is a relationship between the concentration of polymer and the limiting mean particle size. However, the range of values is relatively small, and *Figure 4* shows that the final distribution of sizes was relatively insensitive to the amount of polymer when compared with the initial distribution.

Although the polyethylene particles will act as cavitation nuclei, the concentrations employed here would not be expected to influence the number of cavitation bubbles in the liquid. At higher loadings, there is clearly

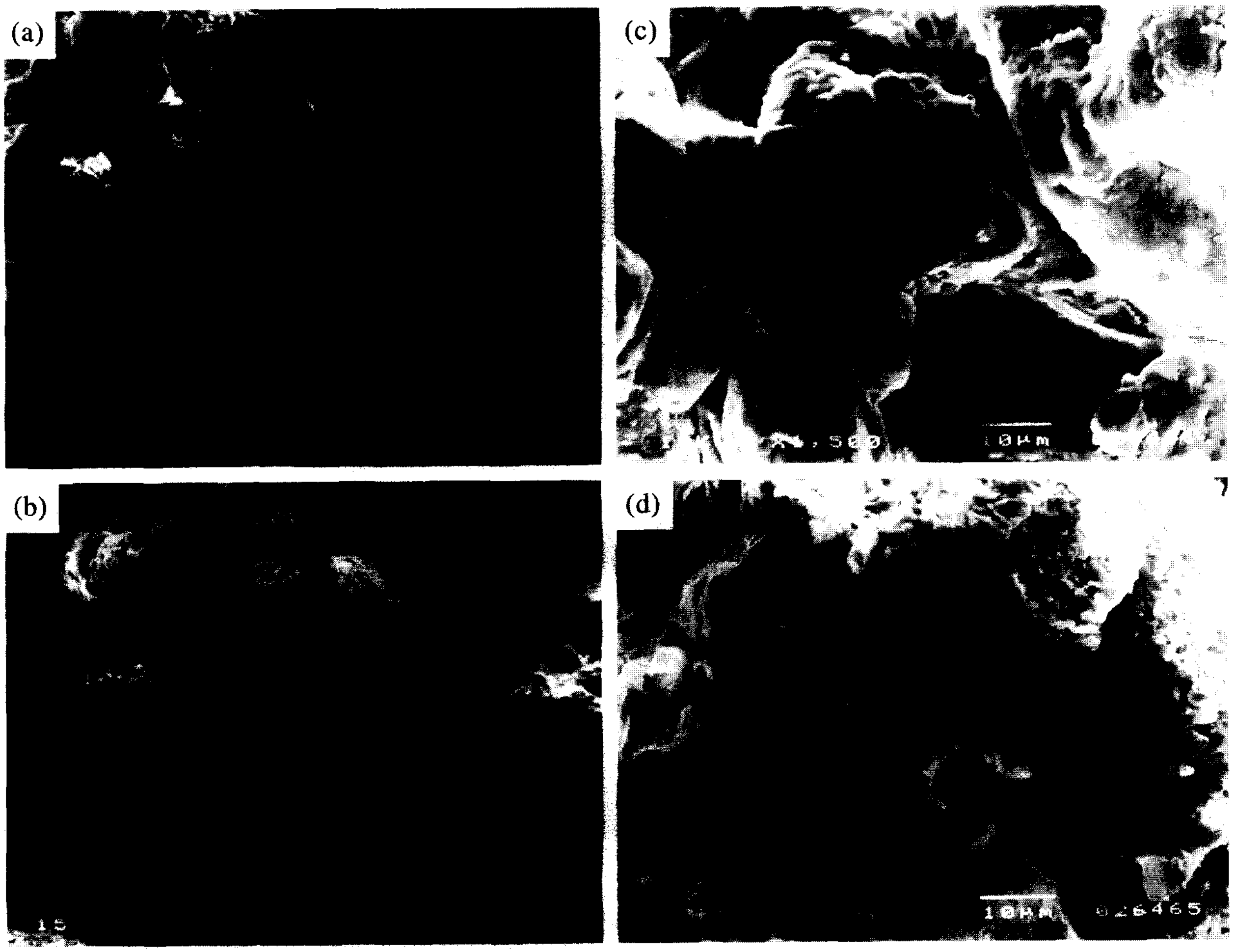

Figure 9 Scanning electron micrographs of PVC, as in *Figure 8*: (a) before sonication, magnification ×500; (b) after sonication, magnification ×500; (c) before sonication, magnification ×1500; (d) after sonication, magnification ×1500

more chance of a particle being in the vicinity of a cavitation bubble and also more surface available on which the microjets could impinge, so that a larger effect and hence smaller final particle size would be expected. Conversely, lower loadings would mean larger volumes available for particle motion to take place and hence a larger effect if particles fragment due to collisions. Hence, these results would seem to suggest a collisional mechanism, although the effect is too small to rule out the other factors that could play a part.

The second polymer chosen for study was polypropylene. The first sample had an average particle size of 159 ± 3 µm, somewhat larger than the polyethylene used above and of the same order as a cavitation bubble. In this case, 5 h sonication had much less effect than on polyethylene, as demonstrated by the size distributions in *Figure 5*. The final average size was 139 ± 3 µm. A second sample having larger particles and a relatively narrow distribution was also used, and the average size was reduced from 381 ±7 µm to 291 ± 5µm by 5 h sonication. In this case, the starting distribution is relatively narrow and it is more difficult to see where the lower limit for fracture occurs, but the breaking-up of the larger particles is clearly demonstrated by the changing distribution in *Figure 6* and also by the optical micrographs shown in *Figure 7* where the presence of considerable amounts of small pieces of material broken off during sonication is clearly evident.

We then turned our attention to polymers with different chemical structures and physical properties, in particular to polymers below their glass transition temperatures. *Figure 8* shows the change of size distribution for sonication of PVC under the same conditions as used above. In contrast to the behaviour of the polyolefins above, the initially quite narrow distribution is considerably broadened. Although the average particle size changes only from 165 µm to 177 µm, the broadening is shown by considering the number distribution of the particles. The starting material is completely within the range 111–270 µm, while in the

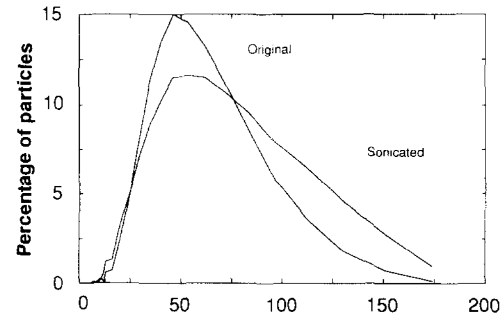

Figure 10 Distribution of particle sizes for sonicated PMMA (sample S)

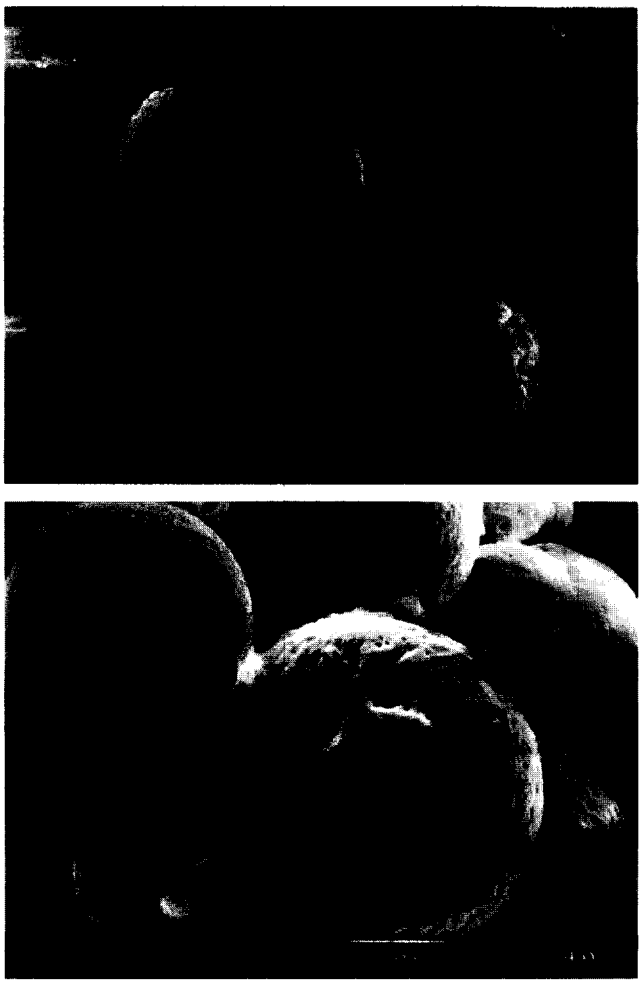

Figure 11 Scanning electron micrographs of PMMA sample S from *Figure 10*: after sonication

sonicated sample, 7.5% of the particles were above this range and 5.9% below. Thus, while some particles fragment, significant agglomeration must also occur. There was nothing significant shown by optical microscopy, but scanning electron microscopy (SEM) revealed changes in the surface morphology of the particles as shown in *Figure 9*. Sonication causes a roughening of the surface with many more small protrusions appearing. Similar observations have been made with metal particles. Collisions between particles of a brittle metal lead to surfaces such as those seen here, while those in a ductile metal lead to a smooth surface[3].

The final polymer investigated was PMMA, which was supplied in the form of glassy spheres. Two samples with different particle sizes averaging $450 \pm 10\,\mu m$ (sample L) and $50 \pm 2\,\mu m$ (sample S) were used. Sonication of the smaller particles under the same conditions as used above produced an increase in their average size to $56 \pm 2\,\mu m$ accompanied by a broadening of the distribution of sizes. *Figure 10* shows that this resulted from an increase in the number of particles $> 80\,\mu m$ rather than any significant fragmentation. As shown in *Figure 11*, the increase is due to the fusing of beads into 'dumbbell' type structures, none of which could be seen in the original sample.

Our interest in promoting reactions at polymer surfaces led us to examine any effect where the surface was much larger than the expected size of the cavitation bubbles. The larger PMMA particles showed no significant change in the size distribution on sonication. However, there is considerable change in the character of the surface. *Figure 12* shows that the initially smooth, shiny surface of the glassy beads becomes opaque after sonication. The higher magnification allowed by electron microscopy, demonstrated in *Figure 13*, indicated that the change was due to a surface roughening with surface indentations and features of the order of 1–2 μm being produced. This is presumably due to small pieces of material being broken off as a result of microjetting against the surface, although it could also result from interparticle collisions.

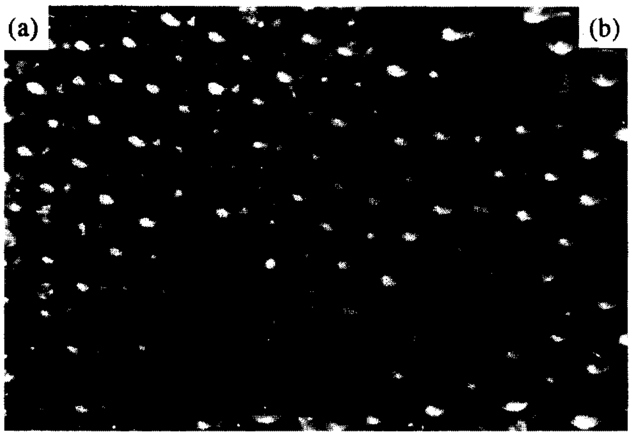

Figure 12 Optical micrograph (magnification ×32) of PMMA sample L: (a) before sonication, (b) after sonication

Any surface changes will certainly be due to microjetting in the final example, that of a polyethylene sheet where clearly no collisional damage was possible. The result is shown in *Figure 14* and demonstrates that, while the original surface is relatively flat and featureless on a micrometer scale, sonication produces considerable roughening with indentations up to $20\,\mu m$ in diameter being produced. However, it is noteworthy that this damage was not visible to the naked eye and no change in the appearance of the film was apparent, suggesting that these features do not penetrate very deeply into the film.

FURTHER DISCUSSION

Our results clearly demonstrate that polymer particles are subject to the same types of agglomeration and fragmentation process that have previously been reported for metal and other inorganic solids as a result of motions induced around collapsing cavitation bubbles. Suslick *et al.* decided that very high temperatures could be generated in metallic powders as a result of interparticle collisions. Clearly this cannot be the case in our systems, as those temperatures would vaporize and clear polymeric materials, which have much lower densities and melting temperatures. However, enthalpies of fusion and melting points are also lower and it seems that the agglomeration observed in PMMA is a result of plastic welding due to the high contact pressures and temperatures generated during head-on collisions.

Further insight can be gained by consideration of the physical properties of the polymers. It should be stressed that the precise values will depend on a number of factors, including the particular processes used during

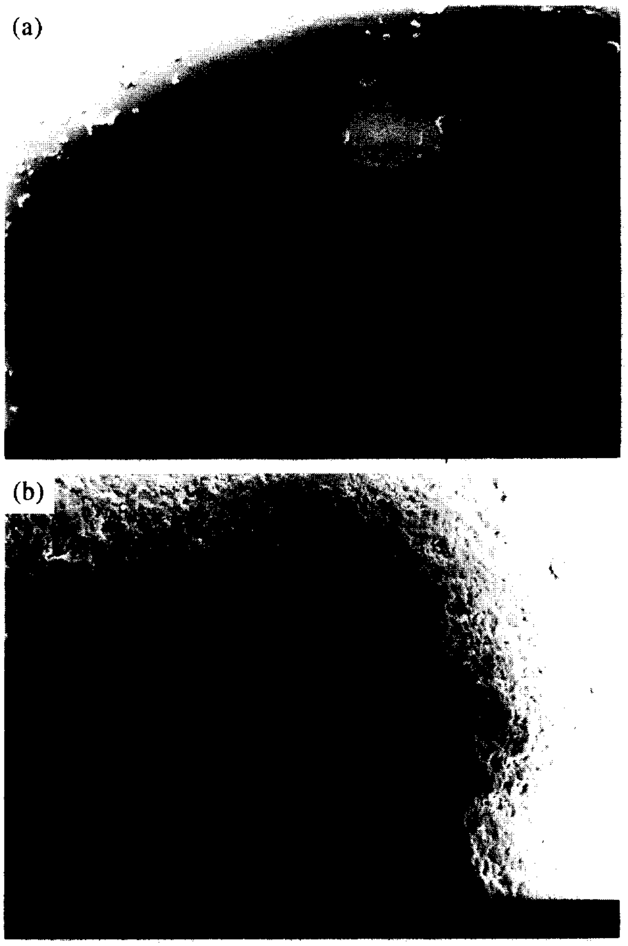

Figure 13 Scanning electron micrographs of PMMA sample L from *Figure 12*: (a) before sonication, (b) after sonication

preparation, and that the impact strength and hardness values are usually measured on bulk rather than powder samples. However, the values[17] included in *Table 1* will suffice for a general discussion in terms of the trends of the data. The impact strength reflects the material's resistance to breakage under high-velocity impact, while the Rockwell hardness and tensile and flexural moduli are measures of how easily the material is deformed.

The table is arranged in increasing order of T_g or strength and decreasing impact strength or extension to break. It also corresponds to decreasing tendency to fragmentation under ultrasound. It might be expected that, if the mechanisms involved arose solely from collisions, then the materials sonicated below their glass transition temperatures would fragment most. Under these conditions they are brittle, whereas PE and PP would deform and might disperse the energy. Conversely, if the shock waves emitted after cavitational collapse were absorbed by the particle or stresses were set up by the jets of liquid impacting their surface, then it would be expected that materials with lower tensile properties would be affected most. Measurements from laser-induced cavitation in water[18] suggest that shock-wave pressures as large as 300 MPa (~ 3000 atm) can be generated on bubble collapse. Thus, it seems that the stresses set up in the particles are sufficient to overcome the low tensile, flexural and breakage of polyethylene and, if the particles are sufficiently large, polypropylene. However, they are too low to deform and break the PMMA particles. Our interpretation of the results is that particles are subjected to stresses from both microjet and collisional impacts. The former have little bulk effect on glassy materials but cause deformation and breakage of materials below T_g. Conversely, this deformation absorbs the stresses caused on collision, whereas with brittle materials this leads to fragmentation of pieces from the surface or agglomeration in the case of head-on collisions. It would clearly be useful if samples of the different polymers having identical particle sizes and distributions could be used to eliminate any effect such as particles with different sizes and masses moving at different speeds. However, these are difficult to obtain except by careful sieving of commercial samples and this will be attempted in our future work. In the case of the polyethylene film, the impact of the microjets is clearly sufficient to deform the polymer and remove some material.

CONCLUSIONS

This work shows that polymer particles undergo fragmentation and agglomeration as well as considerable surface modification when subjected to ultrasound. The observed changes can be correlated with the physical properties of the polymers. While some of the details of the mechanism remain to be confirmed, this preliminary study demonstrates that care must be taken when considering the preparation of latexes or conducting sonochemical reactions with polymer-supported reagents. However, the changes caused at the surface can be exploited for chemical modification, and future publications will detail this.

ACKNOWLEDGEMENTS

We are grateful to the Science and Engineering Research Council for support of this work via a research studentship (to AAC) and the loan of the Malvern particle sizing equipment from the Engineering Board Instrument Pool. Also, we thank BICC Cables Ltd for additional financial support.

Table 1 Physical properties of the polymers

Polymer	T_g (°C)	Impact strength (J m^{-1})	Rockwell hardness	Tensile modulus (10^9 N m^{-2})	Breaking strength (10^5 N m^{-2})	Flexural strength (10^5 N m^{-2})	Extension at break (%)
PE	−120	700	10–40	0.2	1	4.5	400–700
PP	−25	80	100	1.4	3.5	4.9	200–600
PVC	80	43	115	2.6	5	9	5–60
PMMA	100	27	125	3.2	6.5	11	2–10

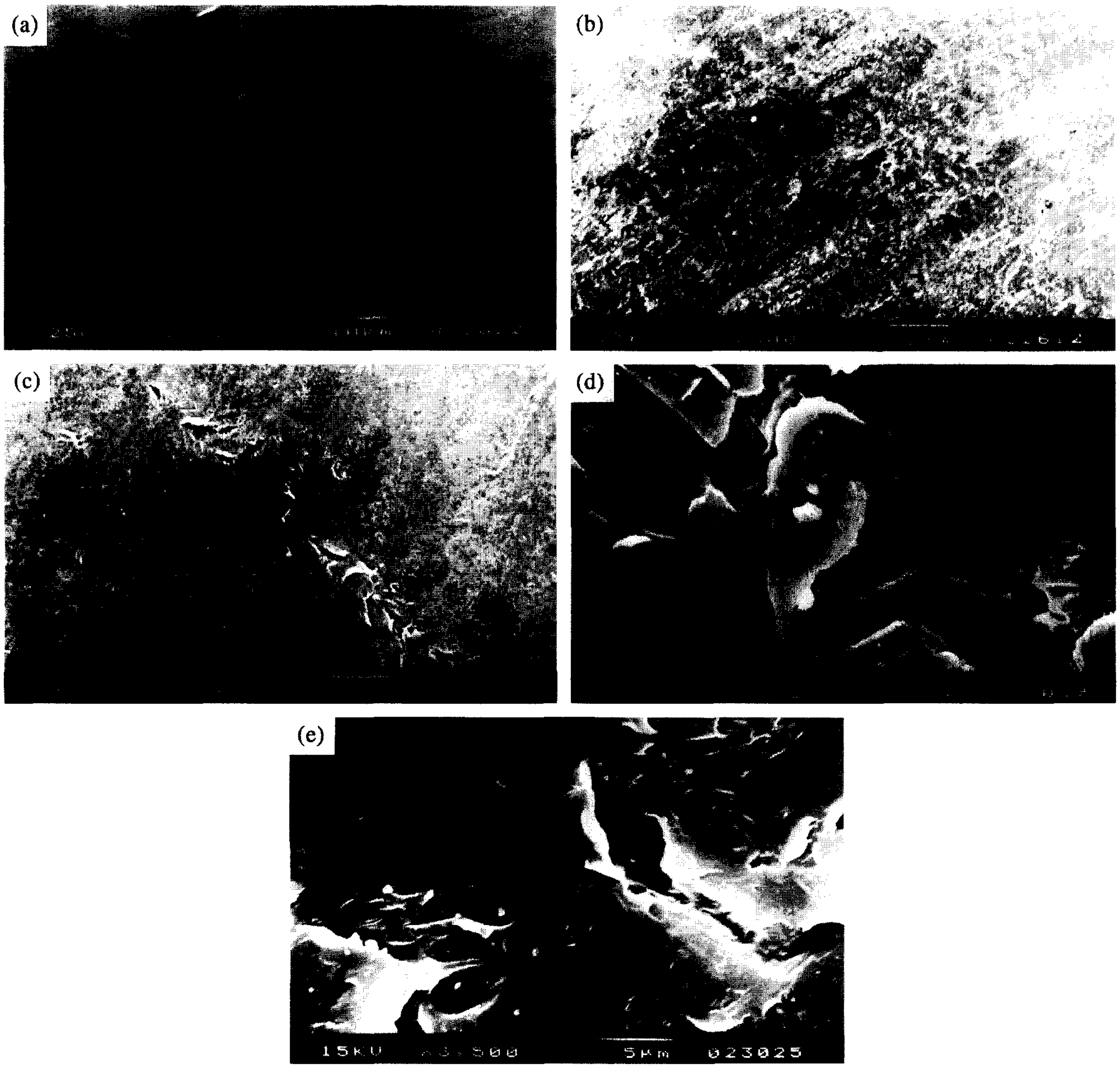

Figure 14 Scanning electron micrographs of polyethylene sheet before and after sonication: (a) before sonication, magnification ×1000; (b) before sonication, magnification ×3500; (c) after sonication, 5 mm from horn tip, magnification ×3500; (d) after sonication, 15 mm from horn tip, magnification ×3500; (e) after sonication, 30 mm from horn tip, magnification ×3500

REFERENCES

1 Price, G. J. (Ed.) 'Current Trends in Sonochemistry', Royal Society of Chemistry, Cambridge, 1992

2 Mason, T. J. and Lorimer, J. P. 'Sonochemistry: Theory, Applications and Uses of Ultrasound in Chemistry', Ellis Horwood, Chichester, 1988

3 Suslick, K. S. 'Ultrasound: Its Chemical, Physical and Biological Effects', VCH Publishers, New York, 1990

4 Doktycz, S. and Suslick, K. S. *Science* 1990, **247**, 1067

5 Pugin, B. and Turner, A. T. *Adv. Sonochem.* 1990, **1**, 81

6 Suslick, K. S., Casadonte, D. J., Green, M. L. H. and Thompson, M. E. *Ultrasonics* 1987, **25**, 56

7 Leighton, T. J. 'The Acoustic Bubble', Academic Press, London, 1994

8 Neppiras, E. A. *Phys. Rep.* 1980, **61**, 159

9 Lauterborn, W. and Hentschel, W. *Ultrasonics* 1984, **24**, 59

10 Lindley, J., Mason, T. J. and Lorimer, P. J. *Ultrasonics* 1987, **25**, 56

11 Price, G. J. *Adv. Sonochem.* 1990, **1**, 231

12 Basedow, A. M. and Ebert, K. H. *Adv. Polym. Sci.* 1977, **22**, 83

13 Price, G. J., ref. 1, p. 87

14 Urban, M. W. and Salazar-Rojas, E. M. *Macromolecules* 1988, **21**, 372

15 Price, G. J. and Smith, P. F. *Polymer* 1993, **34**, 4111

16 Mason, T. J. 'Practical Sonochemistry', Ellis, Horwood, Chichester, 1991

17 van Krevelen, D. W. 'Properties of Polymers', 3rd Edn., Elsevier, Amsterdam, 1990

18 Vogel, A. and Lauterborn, W. *J. Acoust. Soc. Am.* 1988, **84**, 719